Characteristic Basin Formation at Terminations of a Large Transcurrent Fault — Basin Configuration Based on Gravity and Geomagnetic Data

Yasuto Itoh, Shigekazu Kusumoto and
Keiji Takemura

Additional information is available at the end of the chapter

http://dx.doi.org/10.5772/56702

1. Introduction

The formation of a pull-apart basin is a ubiquitous phenomenon associated with transcurrent faulting in the Earth's upper crust (e.g., [1]). Because an oblique mode of subduction provokes the detachment and transcurrent motion of a forearc crustal sliver [2], numerous pull-apart basins develop on active plate margins.

Southwest Japan is an island arc that has long been under the influence of the oblique subduction of oceanic plates. Figure 1 delineates its bisecting fault, the Median Tectonic Line (hereafter referred to as MTL). Regional pull-apart basins related to sinistral motion of the MTL during the late Cretaceous were described by Noda and Toshimitsu [3]. Vigorous sinistral faulting also caused regional wrench deformation of the adjoining terranes [4]. The northwestward motion of the Philippine Sea Plate, depicted as a positive gravity anomaly (red-colored) portion within the Pacific Ocean in Figure 1, resulted in dextral slips on the MTL since the Pliocene. Although the recent activity of the MTL is key to understanding the neotectonic regime of southwest Japan [5], basin-forming processes along the regional fault system have not been fully described.

The authors attempt to present a quantitative description of sedimentary basins at the western and eastern terminations of the MTL, namely, the Beppu-Iyo Basin and Osaka Basin, respectively (Figure 1). As shown by negative gravity anomalies, they are enormous depressions filled by recent clastics. Seismic surveys in the study areas became popular in recent decades, but interpretation has not reached a mature stage. Thus, we utilize gravimetric methods for estimating their morphology and volume. Geomagnetic anomaly modeling helps us to identify subsurface constituents of the sedimentary basins. Additionally, the evolutionary processes of the basins are argued based on geologic information. This is a multidisciplinary case study of basins ahead of a comprehensive visualization of the basin interior with seismic information.

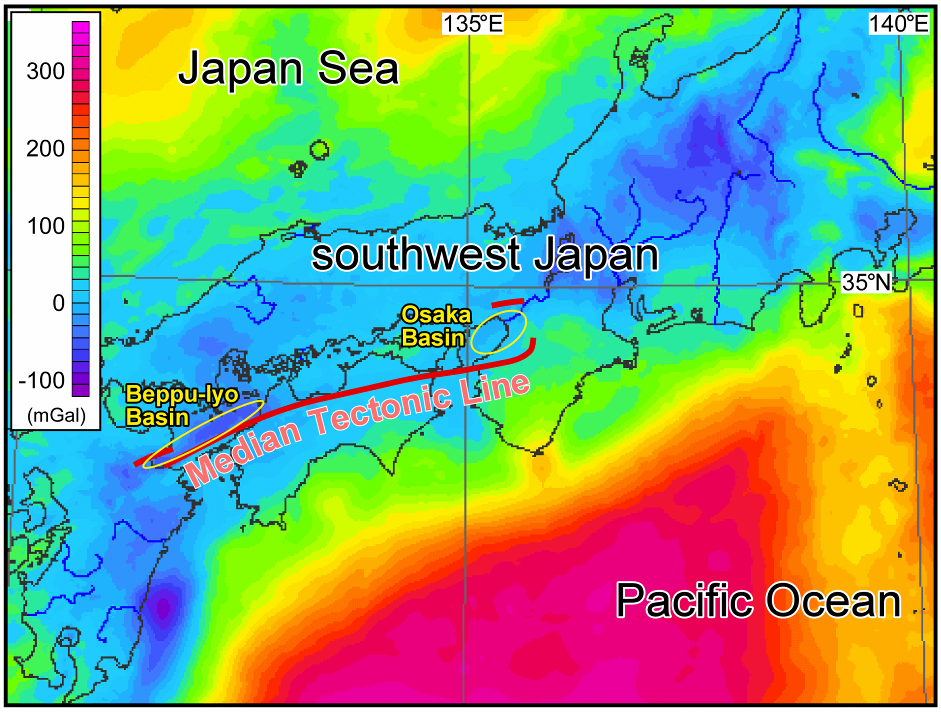

Figure 1. Index map of the studied basins. Base map shows Bouguer gravity anomaly [6]. Bouguer density is 2670 kg/m^3. The northern part of the Philippine Sea Plate is depicted as a positive gravity anomaly (red-colored) portion within the Pacific Ocean. Shape of an oceanic plate is generally delineated by positive Bouguer anomaly in ocean, because an area of deep water is accompanied by positive gravity values as a result of correction procedures (cf. Y. Itoh, K. Takemura and S. Kusumoto in this book)

2. Volumetric analysis

Volume estimation of the basins is necessary in order to consider the mass balance of the upper crust around the island arc. Utilizing a gravity database [6], we present the analytical results for the Beppu-Iyo and Osaka Basins in the following sections.

2.1. Beppu-Iyo Basin

The large depression of the Beppu-Iyo Basin is divided into the Beppu Bay (west) and Iyonada Sea (east) areas by a relative high of the Bouguer anomaly. Beppu Bay is a younger part of an extensive tectonic depression, the Hohi Volcanic Zone, which has been developed since the Pliocene [7]. As for the Beppu Bay basin, active trace of the MTL is terminated around southwestern coast of the bay (e.g., [7]). Right-stepping lateral faults are aligned on the northern corner of the bay, and the parallel two fault strands are connected by normal listric faults constituting a rhomboidal depression surrounded by the faults [7]. These structural patterns are characteristic for releasing bend of strike-slip fault.

The Iyonada Sea is characterized by a remarkable negative gravity anomaly [8,9], but its origin has not been discussed so far. In contrast with the Beppu Bay basin, ambiguous points remain in the formation mechanism of the extensive Iyonada Sea depression. Paired dextral fault is not identified, and the basin is not regarded as an elongate sag in an area of propagation of lateral fault terminations because the sag is buried by recent sediments (Age assignment of a sedimentary unit upon the basin margin is presented in a following section.) simultaneous with those in the western termination of the MTL (Beppu Bay; [7]).

2.1.1. Beppu Bay

Kusumoto et al. [10] determined a three-dimensional subsurface structure around Beppu Bay on the basis of gravimetric data. We adopt their structural model and estimate the volume of the sedimentary basin. Figure 2 is a compiled map of the Hohi Volcanic Zone. The volume of the basement depression is calculated by the Gauss-Legendre numerical integration [11], from depth data given on the mesh with a 10 km interval, and is 4.1×10^3 km^3.

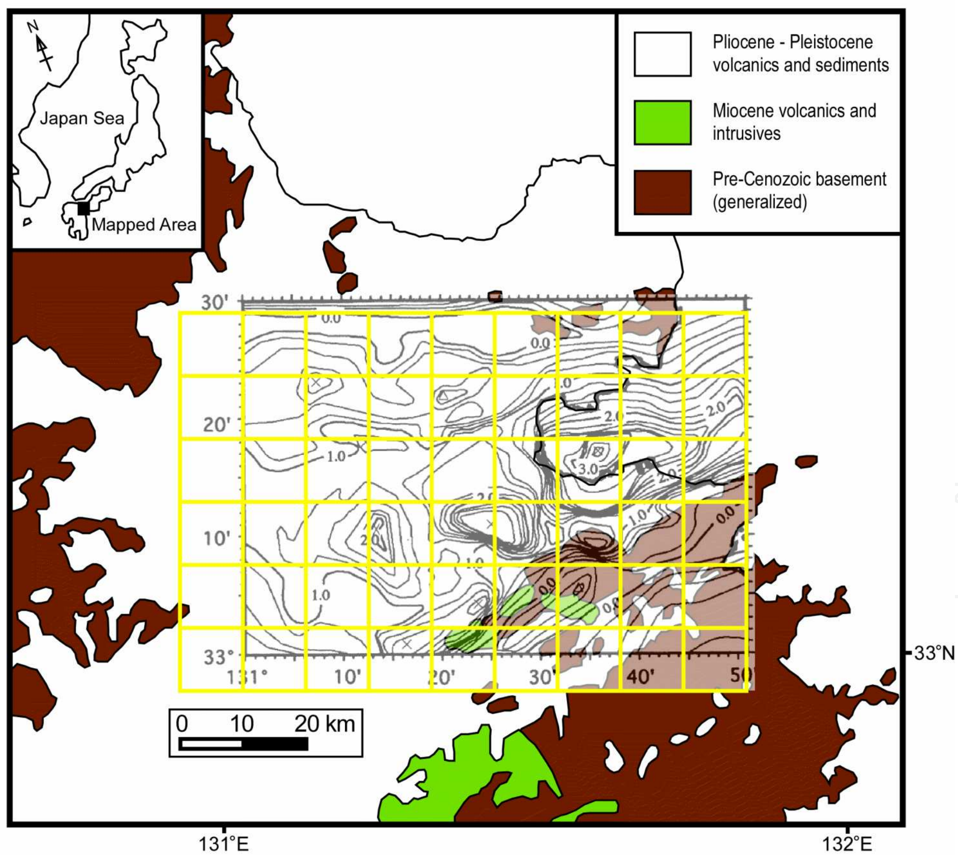

Figure 2. Simplified geology around the Hohi Volcanic Zone including Beppu Bay. Overlain basement structural contours are based on gravity anomaly modeling after Kusumoto et al. [10]. Grid shows data points for volumetric analysis

2.1.2. Iyonada Sea

Figure 3 is a Bouguer anomaly map around the Iyonada Sea with two-dimensional gravity modeling lines (1−10). Although a previous study [9] assumed there to be three units with different densities in the basement rock, its geologic context still remains ambiguous. Therefore we adopted a simple two-layered (sediment and basement) model. We applied Talwani's method [12] in order to estimate two-dimensional subsurface structures and assumed that the each structure at both ends of each profile was infinity to the depth. As shown in Figure 4, the remarkable elongate depression has a profile common with a half-graben, implying a tensile stress state. An isopach map indicating the top basement structure (Figure 5) demonstrates that the deepest part of the basin reaches 4 km from mean sea level. The volume of the basement depression is calculated by the Gauss-Legendre numerical integration [11], from depth data given on the mesh with a 10 km interval, and is 7.2×10^3 km^3.

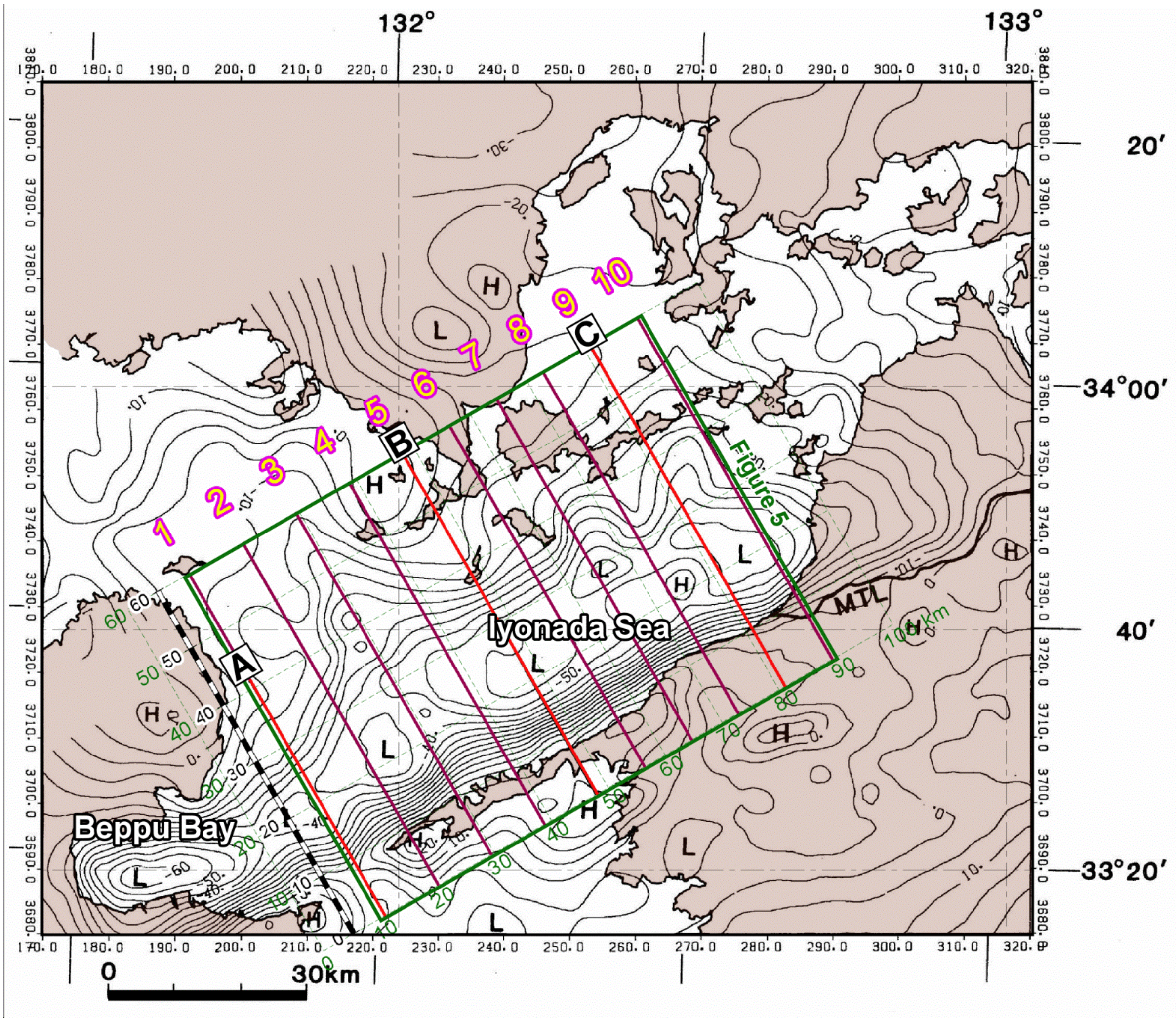

Figure 3. Bouguer gravity anomaly map around the Beppu-Iyo Basin [9]. Bouguer density is 2670 kg/m³. Contour interval is 5 mGal. Lines 1 to 10 are for 2-D gravity anomaly modeling in the Iyonada Sea. A, B and C show previous modeling lines [9]

http://dx.doi.org/10.5772/56702

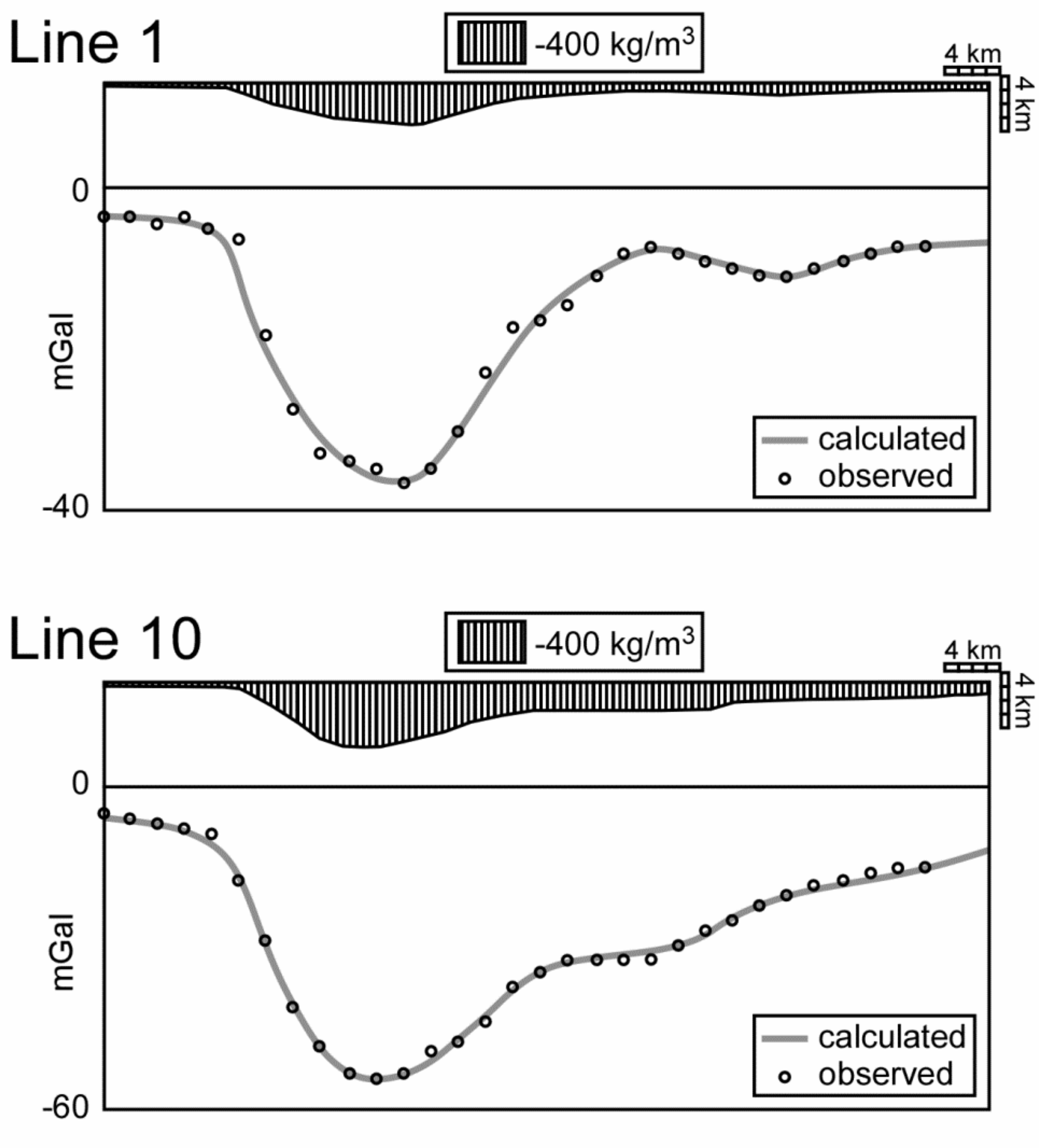

Figure 4. Examples of Bouguer anomaly profiles calculated for the two-layer models. See Figure 3 for line location

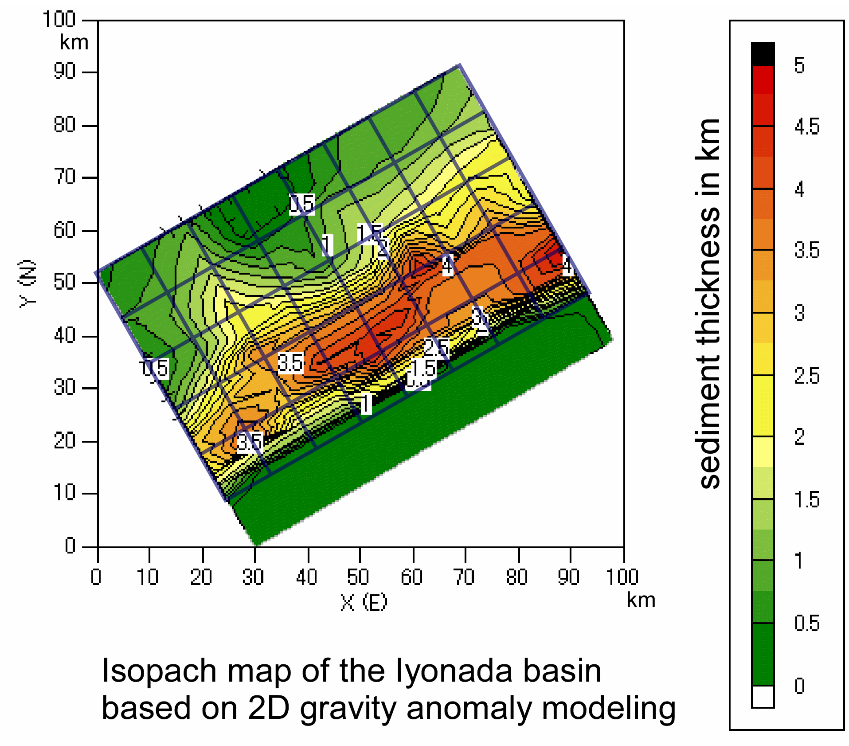

Figure 5. Isopach map of the Iyonada Basin based on 2D gravity anomaly modeling, indicating basement structure of the Iyonada Sea. See Figure 3 for mapped area. Grid shows data points for volumetric analysis

2.2. Osaka Basin

The active trace of the MTL tends to shrink compared to the older phase of faulting. Its eastern termination is now around 136ºE with a length of active segment of 400 km, whereas the Cretaceous MTL as a significant geological break reached ca. 140ºE with a total length of 800 km [13]. The Arima-Takatsuki Tectonic Line (E-W trending fault on the northern flank of the Osaka Basin; Figure 1) is the unique parallel fault around the shrunken eastern termination having comparable dextral slip rate during the Quaternary [14]. Although this fault alignment should act as a confining bend, the area is characterized by recent vigorous basin formation around the Osaka Bay. We, therefore, attempt to simulate the deformation pattern introducing effect of reverse slips on secondary faults which show complex arrangement as a result of longstanding differential motion of crustal blocks (cf. Y. Itoh, K. Takemura and S. Kusumoto in this book) in a following section.

A regional structural model around the eastern termination of the MTL has not been shown because complicated basin morphology does not allow two-dimensional modeling. Thus, we estimated mass deficiency from the gravity anomaly data of the Osaka Basin given on the mesh with a 5 km interval (Figure 6) by Gauss's theorem [15]:

$$\Delta M = \frac{1}{2\pi G} \iint_{-\infty}^{\infty} \Delta g(x,y) dxdy \tag{1}$$

Here, $\Delta g(x, y)$ is the gravity anomaly data given on an xy mesh with a constant interval. G, π and ΔM are the universal gravitational constant, circular constant and deficiency/excess of mass, respectively. Next, a first approximation of the volume of the sedimentary basin was calculated, from the estimated deficiency of mass by assuming a density contrast of 400 kg/m^3 between sediment and basement, to be 9.1×10^2 km^3.

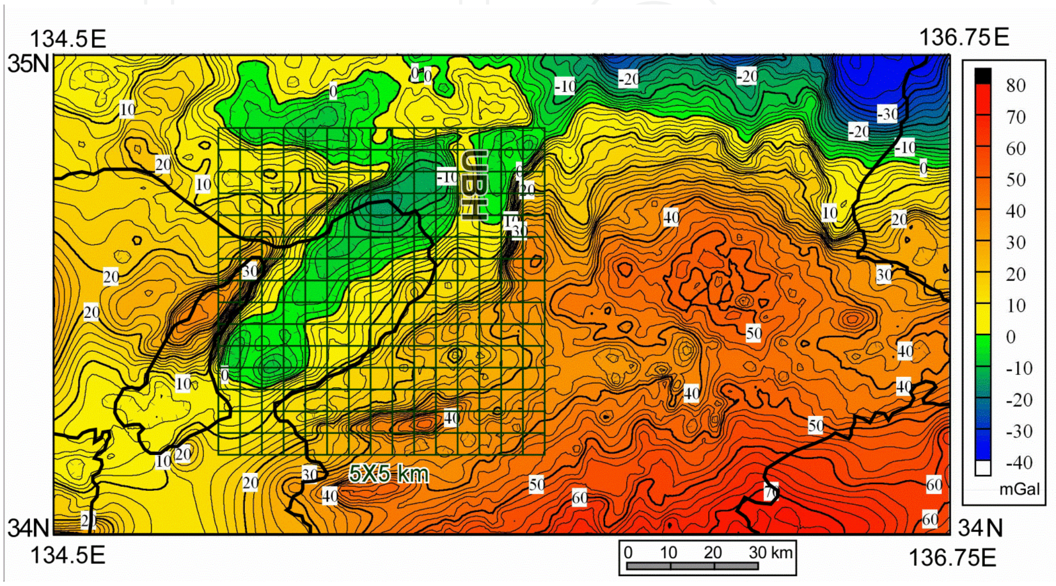

Figure 6. Bouguer gravity anomaly map [6] around the Osaka Basin. Bouguer density is 2670 kg/m^3. Grid shows data points for volumetric analysis. UBH is the Uemachi Basement High in the Osaka Basin

The present result indicates that the total volume of the sedimentary basin at the western end of the MTL is 10 times larger than that of the eastern counterpart. It may be attributed to a difference in the mechanism of basin formation between releasing and confining steps of strike-slip faults, which will be discussed later.

3. Sedimentation process of the Beppu-Iyo Basin

Itoh et al. [7] demonstrated that the Hohi Volcanic Zone, including the Beppu Bay, has shifted its depocenter according to the transition of active segments of major faults, among which the MTL acted the most significant role for the development of tectonic sedimentary basin. As for the Iyonada Sea, which lacks seismic or drilling survey subsurface information, we aim at finding a temporal change in sediment supply pattern deduced from lithologic observation of an adjoining onshore sedimentary unit.

Figure 7 shows a geologic map around the eastern part of the Iyonada Sea [16]. It is known that a conspicuous sedimentary unit known as the Gunchu Formation is distributed along the northwestern coast of the Shikoku Island [17], which is a non-marine deposit containing abundant plant remains and has a steep homoclinal structure affected by the Quaternary activity of the MTL running along the southern margin of the Iyonada Sea [18]. The Middle Member of the Gunchu Formation contains a considerable amount of crystalline schist gravels that were derived from the Sanbagawa metamorphic belt [19]. Its sedimentological description, however, has not been reported. Therefore the authors present the results of our preliminary geologic survey and chronological analysis in the following sections.

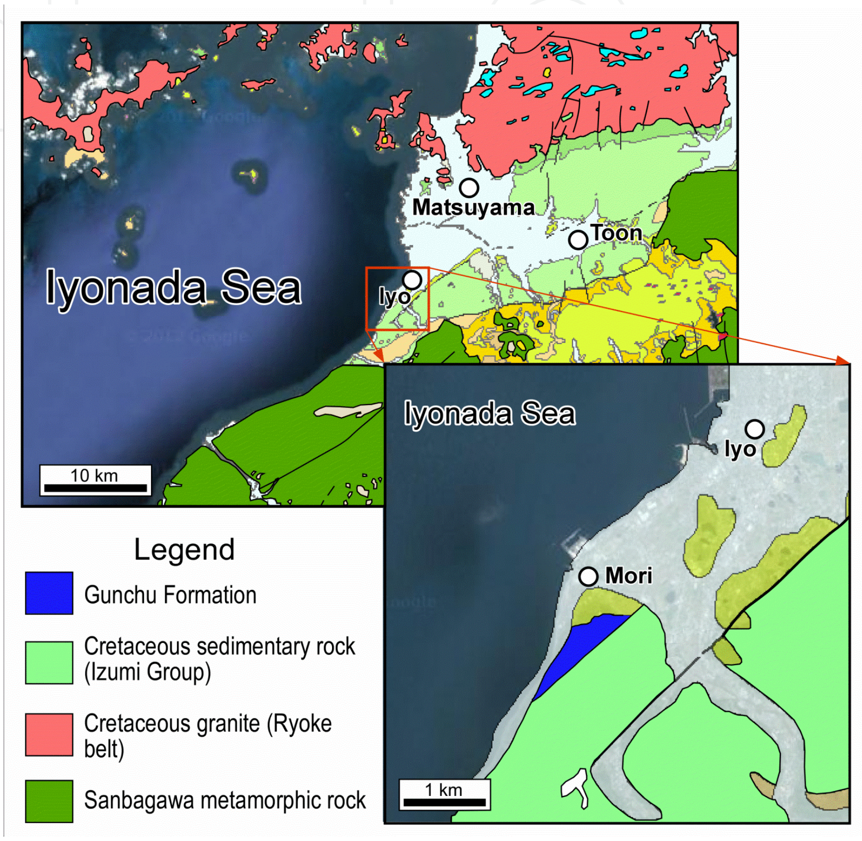

Figure 7. Geological index around the eastern part of the Iyonada Sea [16]

sample	mineral	No. of crystals	Spontaneous track		Total U count		r	P (χ^2) (%)	U (ppm)	Age±1σ (Ma)	Method
			ρ_s (cm^{-2})	N_s	ρ_u (cm^{-2})	N_u					
granite	zircon	30	1.11×10^7	4938	3.48×10^8	154845	0.856	0	280	77.9±6.1	IS

Table 1. Fission-track age of granite pebbles contained in basal part of the Gunchu Formation*r* is correlation coefficient between ρ_s and ρ_u. P (χ^2) is the probability of obtaining χ_2-value for ν degrees of freedom (where ν = No. of crystals - 1). IS means internal surface

3.1. Provenance and sedimentary structure

Figure 8 shows results of the geologic survey of the Middle Member of the Gunchu Formation along the coastal section. It is clear that the composition of gravels fluctuates along the section in response to changes in lithology. The content of schist gravel is related to sediment supply from the Outer Zone, a geologic zone on the southern side of the MTL. The paleocurrent direction, based on the imbrication structure of gravels, also shows considerable variation. It seems that the E-W elongate trough of the Iyonada Sea was alternately buried by the westward and northward influx of clastics. Further facies analysis would help provide an understanding of the sedimentary system of the pull-apart basin.

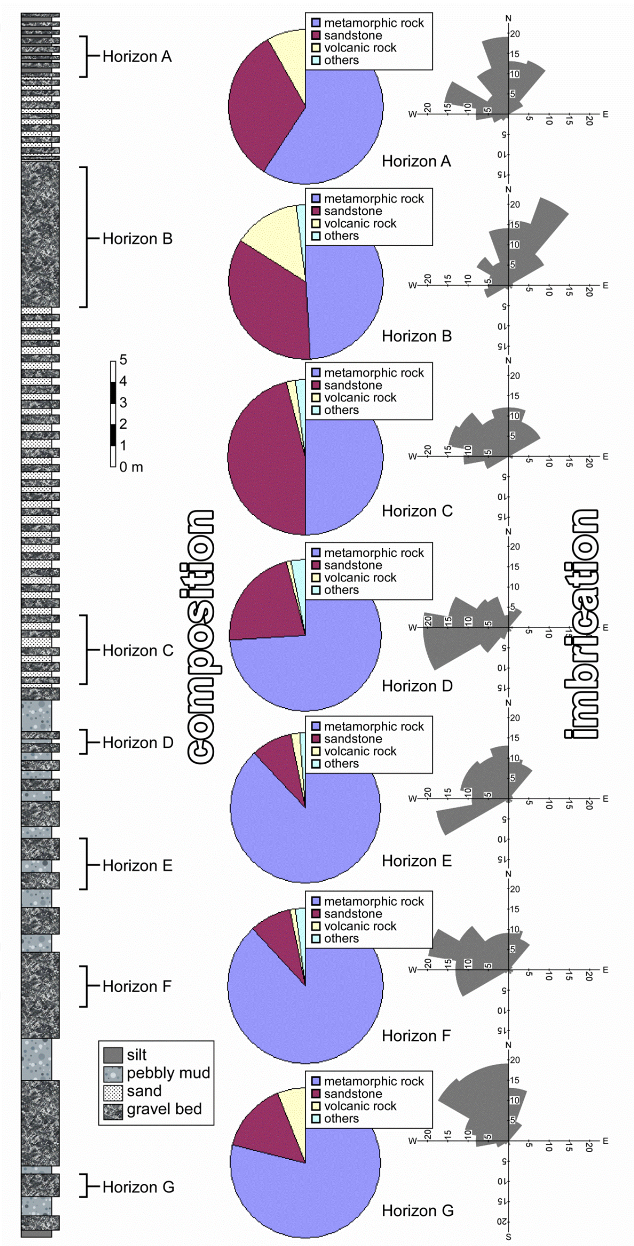

Figure 8. Sedimentological description of the Pleistocene Gunchu Formation. Left: Lithologic column of the Middle Member of the Gunchu Formation. Center: Gravel composition of selected horizons. Right: Rose diagrams showing paleocurrent directions (downcurrent directions) of the selected horizons measured using imbricate structure of gravels. Number of data is 100 for each measured horizon

3.2. Chronology

Kitabayashi et al. [20] executed fission-track dating of an ash layer intercalated in the Lower Member of the Gunchu Formation, and obtained an age of 2.2 Ma. Thus the subsidence and burial of the huge depression of the Beppu-Iyo Basin seems to be a recent event, maybe in response to an accelerated slip rate on the MTL. From the viewpoint of sediment provenance, we executed fission-track dating for pebble samples. It is noted that the Lower Member of the Gunchu Formation is lacking in schist gravels, and is characterized by sporadic granite pebbles. Table 1 and Figure 9 suggest that the granite pebbles were derived from the Cretaceous Ryoke intrusive rocks, which are distributed on the northern side of the MTL (Figure 7). Cessation of sediment supply from the northern terrane is thought to reflect entrapment of clastics in a deepening tectonic basin, and the succeeding emergence of voluminous schist gravels may correspond to an episodic uplift of the forearc sliver. Thus the drastic change in the pattern of sediment supply is a key to describe development processes of the tectonic basin.

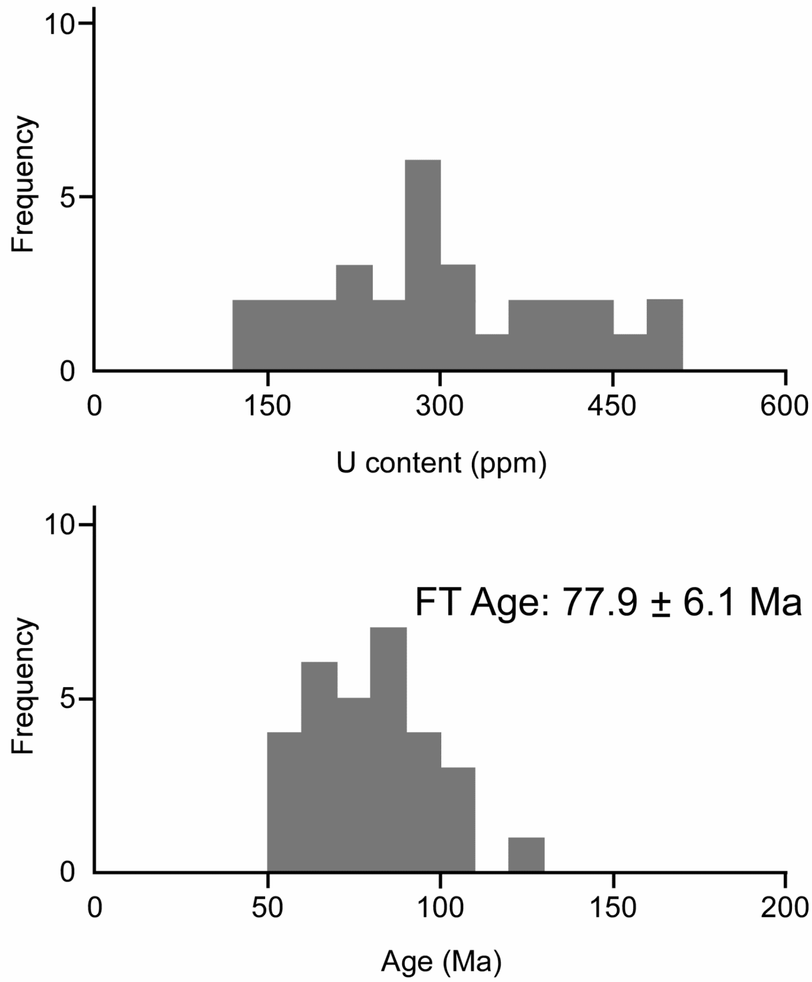

Figure 9. Result of fission-track dating of granite pebbles contained in the lowermost part of the Gunchu Formation. See Table 1 for detailed analytical data

http://dx.doi.org/10.5772/56702

4. Development of the Osaka Basin

In contrast to the simple half-graben on the western end of the MTL, the Osaka Basin at the eastern end is characterized by a complicated subsurface morphology reflected in the pattern of the gravity anomaly [21,22] (Figure 10). We argue a mechanism of basin formation based on numerical modeling, describe the seismic reflection profile showing the deformation pattern during the development of the basin, and interpret the origin of a concealed geologic unit on the basis of gravity and geomagnetic anomaly modeling in the following sections.

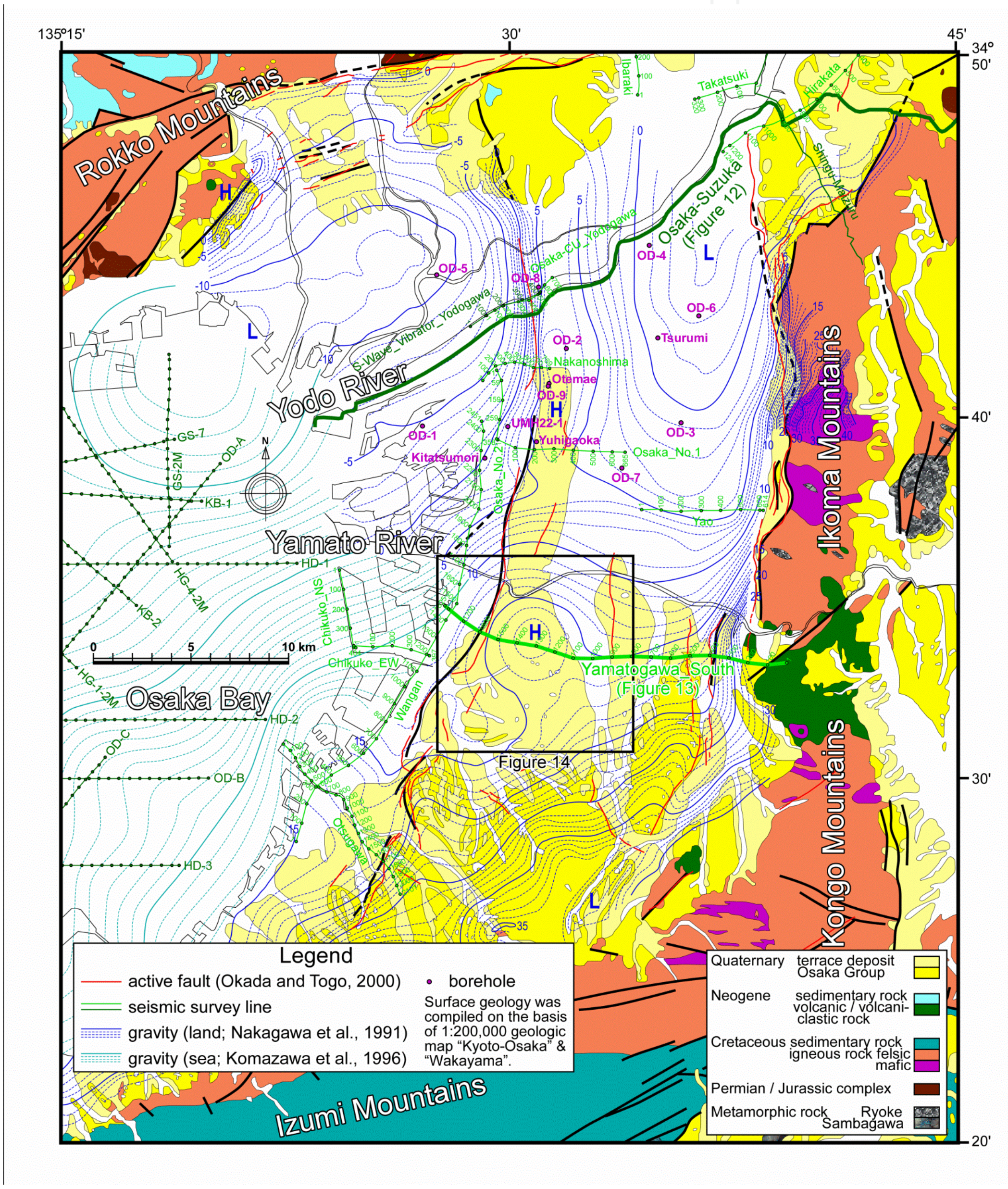

Figure 10. Geologic and geophysical database of the Osaka Basin (mainly for land area). Gravity contour is compiled after Nakagawa et al. [21] and Komazawa et al. [22]

4.1. Paradox of basin formation at a confining bend of a fault

Figure 11 delineates the deformation scheme at stepping parts of strike-slip faults. Generally speaking, a depression is formed at a right-stepping part of a dextral fault (Figure 11a), whereas an upheaval is formed at a left-stepping part of a dextral fault (Figure 11b). The MTL and the Arima-Takatsuki Tectonic Line (Figure 11c) are considered to act as a confining left-step of the regional dextral fault. However, geologic information shows that the Osaka Basin is a site of Quaternary basin formation. In order to solve the paradox, Kusumoto et al. [23] executed dislocation modeling for assessment of the vertical displacement at a complex termination of a strike-slip fault. They found that actual basin morphology could be restored by introducing reverse motions to secondary faults as shown in Figure 11c. The simulated deformation field predicts that a relative basement high, which corresponds to the Uemachi Basement High (UBH) in Figure 6, emerges within a depression surrounded by the modeled active faults.

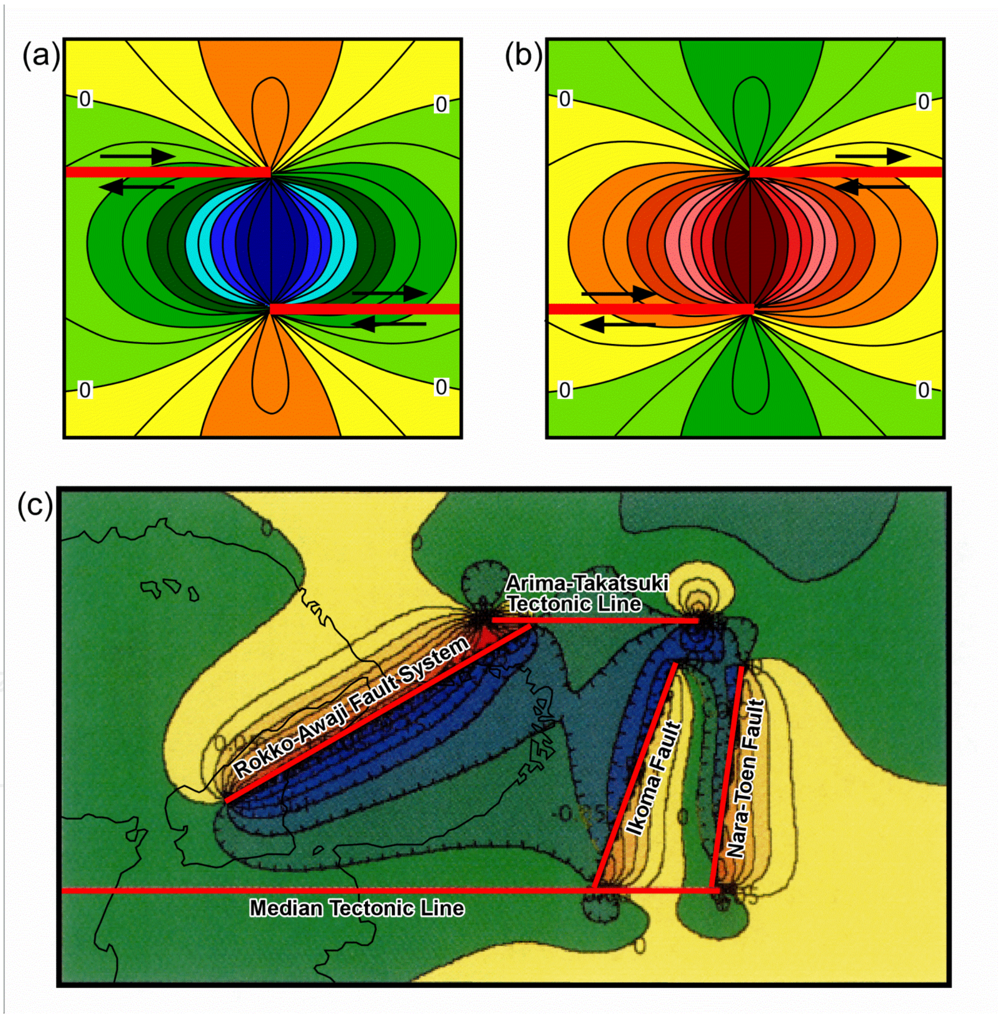

Figure 11. Architecture of numerical modeling of the formation of the Osaka Basin [23]. (a) Normalized vertical displacement at a releasing bend of a strike-slip fault. (b) Normalized vertical displacement at a confining bend of a strike-slip fault. (c) Dislocation model of the Osaka Basin. Red lines are major faults adopted for the modeling. Warm and cold color gradations indicate upheaval and subsiding areas, respectively

http://dx.doi.org/10.5772/56702

4.2. Seismic interpretation

Figure 12 is an E-W seismic reflection profile across the northern part of the Osaka Plain (land area of the Osaka Basin) [24]. Although the internal structure of the sedimentary basin should be discussed with detailed stratigraphic control utilizing borehole information in the future, it is noted that faults within the profile show normal and reversed displacements in the western and the eastern portions, respectively. A close-up of the western portion is characterized by a master normal fault accompanied by a collapsed anticline on its downthrown side. It coincides with the area of relative upheaval in the numerical modeling (shown by warm-colored portions within the fault-bounded basin in Figure 11c), and accords with the actual extensional structure, which is generally expected around an area of upheaval in the modeling of crustal deformation.

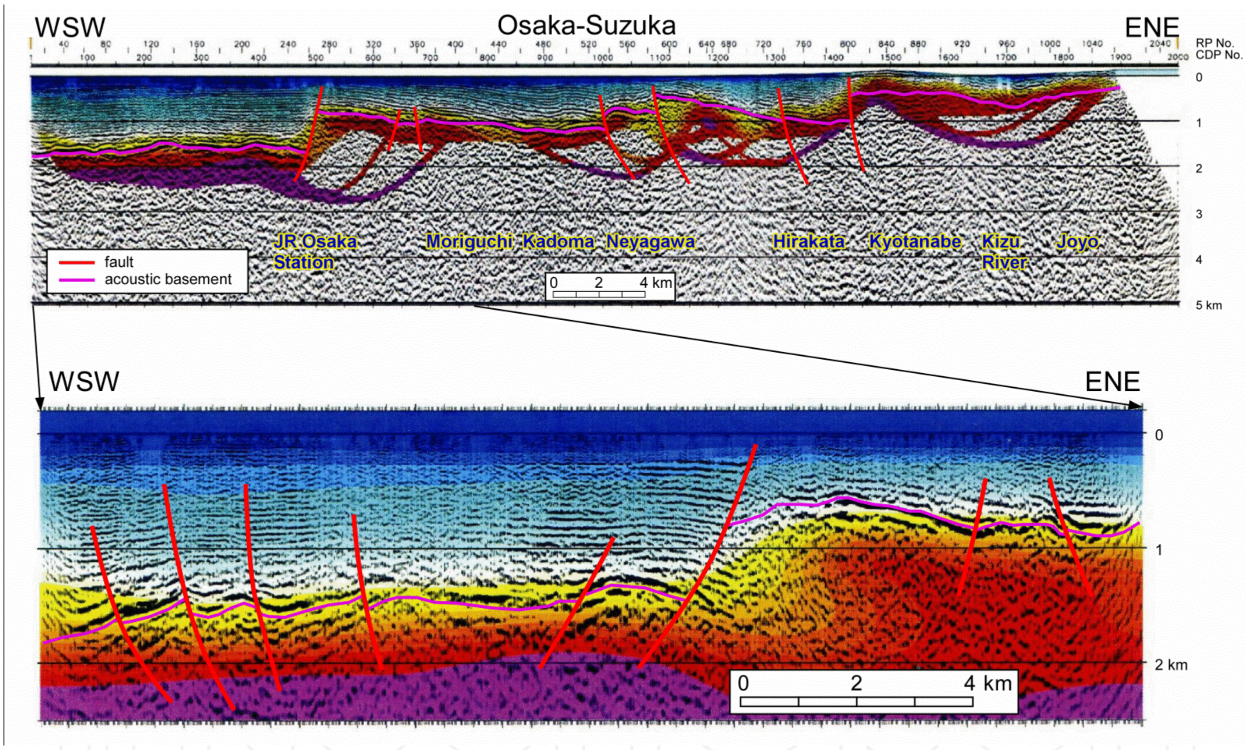

Figure 12. A depth-converted seismic profile (Osaka-Suzuka) crossing the northern part of the Osaka Plain [24]. See Figure 10 for line location

Seismic data indicate a large diversity in structural attitudes in the Osaka Basin. Figure 13 is an E-W seismic profile across the southern part of the Osaka Plain [25]. Remarkable vertical displacement with a steep gradient of the Bouguer gravity anomaly is observed at the easternmost part of the profile, and interpreted as the southern part of the Ikoma fault system (Figure 11c). A strong reflection in the eastern part of the basin is correlated with the Miocene volcanic surface based on surface geology along the survey line. It is noteworthy that a unit showing similarity in reflection pattern with the volcanic rocks is buried on the upthrown side of a reverse fault around the western part of the section. As the unit is accompanied by a positive gravity anomaly [21] and geomagnetic anomaly [26], we will construct three-dimensional models for the subsurface seismic unit.

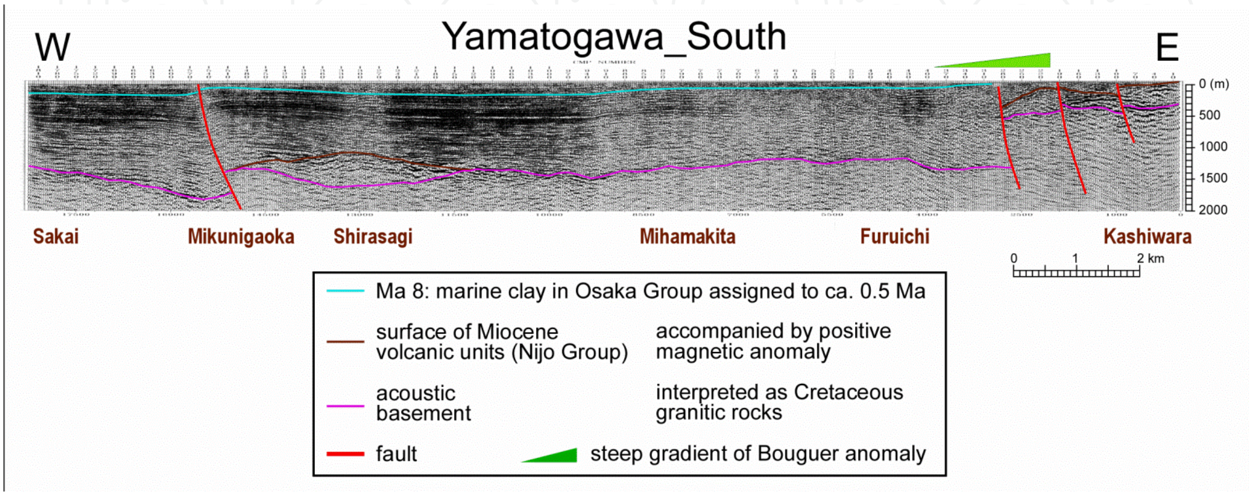

Figure 13. A depth-converted seismic profile (Yamatogawa South) crossing the southern part of the Osaka Plain [25] without vertical exaggeration. See Figure 10 for line location

4.3. Anomaly modeling

Middle Miocene volcanic rocks, collectively named the Nijo Group, are exposed in a hilly province upon the eastern margin of the Osaka Basin. It has been studied from stratigraphic (e.g., [27]) and paleomagnetic (e.g., [28]) points of view, and regarded as a volcanic product formed just after the clockwise rotation of southwest Japan related to the opening of the Japan Sea.

We assumed that conspicuous gravity and geomagnetic anomalies in the southern Osaka Plain are caused by a buried middle Miocene volcano, and estimated its three-dimensional structure based on Talwani's methods [29,30]. Figure 14 summarizes the modeling parameters. We assumed that the body of the volcano is magnetized parallel to the Earth's axial dipole field because the majority of the Nijo Group acquired its thermoremanent magnetization during the normal polarity Chron after the Miocene clockwise rotation of southwest Japan. As shown in Figure 14, gravity and geomagnetic anomalies are successfully simulated on the assumption of a conical volcano on the base of the sedimentary basin. In the Osaka Basin, there are isolated positive Bouguer anomalies associated with magnetic signatures from place to place. Combined anomaly modeling is a useful tool to estimate the origin of subsurface units in advance of a comprehensive interpretation of seismic data.

http://dx.doi.org/10.5772/56702

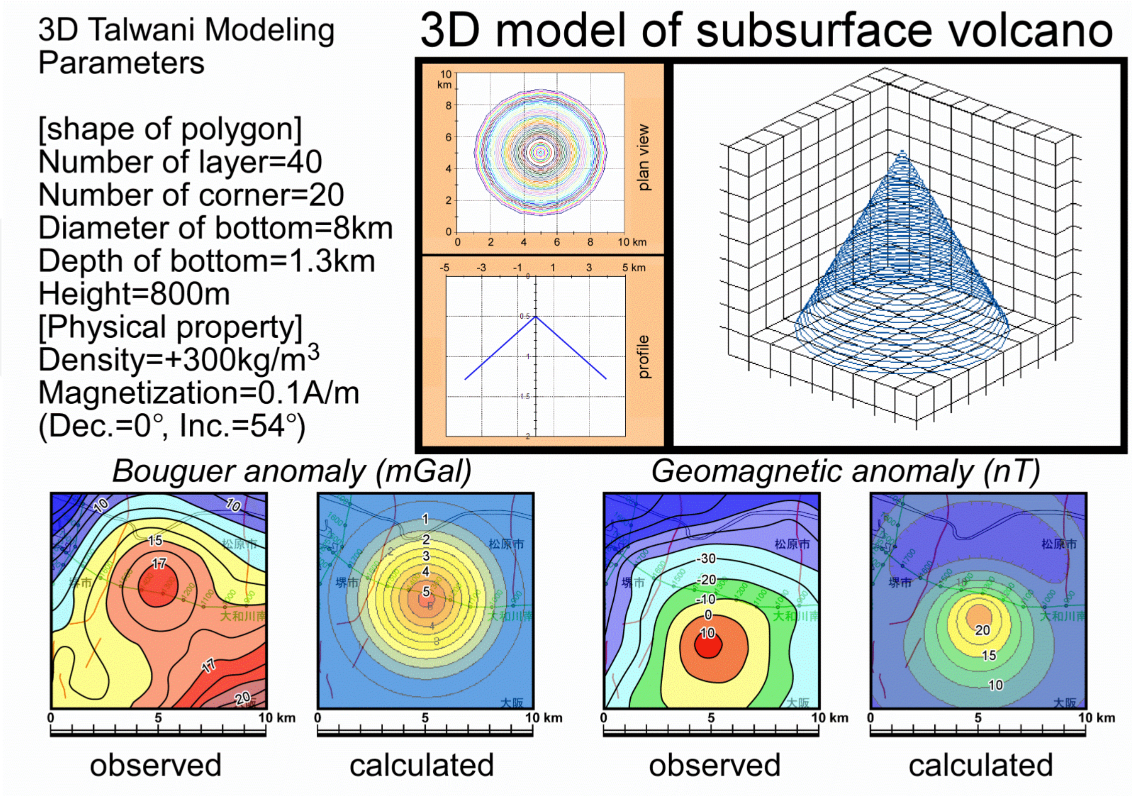

Figure 14. Three-dimensional gravity and geomagnetic modeling of subsurface structure in the southern Osaka Plain. See Figure 10 for mapped area

5. Summary

An integrated geophysical study of sedimentary basins was executed on an active plate margin. Volumes of conspicuous depressions upon both terminations of the Median Tectonic Line (MTL), a dextral bisecting fault of the southwest Japan arc, were estimated by means of gravimetric methods. The western end of the MTL and its secondary faults constitute a releasing step and form a gigantic composite depression of the Beppu-Iyo Basin and has been developed since the Pliocene. Sedimentological and chronological investigation revealed that the major constituent, the Iyonada Sea depression, was rapidly buried during the Quaternary by clastics derived from different geologic terrains. On the other hand, the eastern end of the MTL is a site of basin formation (Osaka Basin), even though the fault architecture is regarded as a confining step. Numerical modeling showed that a combination of major strike-slip and secondary reverse faults can provoke complicated ups and downs within an area surrounded by faults. The stress regime predicted through the modeling of the vertical displacement was concordant with the deep structure of the basin visualized by seismic interpretation. Although the present study area is not accompanied by sufficient geologic evidence of a deep basin interior provided by drilling survey, geomagnetic anomaly modeling successfully delineated a buried volcanic unit, which was anticipated from the viewpoint of regional geology.

Acknowledgements

The authors are grateful to O. Takano for his constructive review; an early version of the manuscript was substantially improved by his comments.

Author details

Yasuto Itoh[1], Shigekazu Kusumoto[2] and Keiji Takemura[3]

1 Graduate School of Science, Osaka Prefecture University, Osaka, Japan

2 Graduate School of Science and Engineering for Research, University of Toyama, Toyama, Japan

3 Graduate School of Science, Kyoto University, Kyoto, Japan

References

[1] Aydin A, Nur A. Evolution of pull-apart basins and their scale independence. Tectonics 1982; 1: 91-105.

[2] Fitch TJ. Plate convergence, transcurrent faults, and internal deformation adjacent to southeast Asia and the western Pacific. Journal of Geophysical Research 1972; 77: 4432-4460.

[3] Noda A, Toshimitsu S. Backward stacking of submarine channel-fan successions controlled by strike-slip faulting: The Izumi Group (Cretaceous), southwest Japan. Lithosphere 2009; 1: 41-59.

[4] Wang CL. Metamorphism and tectonics of the Sanbagawa Belt in northwestern Kii Peninsula, southwest Japan. PhD thesis. Kobe University; 1997.

[5] Huzita K. Role of the Median Tectonic Line in the Quaternary tectonics of the Japanese islands. Memoir of Geological Society of Japan 1980; 18: 129-153.

[6] Gravity CD-ROM of Japan, Ver. 2, Digital Geoscience Map P-2. [CD-ROM] Tsukuba: Geological Survey of Japan; 2004.

[7] Itoh Y, Takemura K, Kamata H. History of basin formation and tectonic evolution at the termination of a large transcurrent fault system: deformation mode of central Kyushu, Japan. Tectonophysics 1998; 284: 135-150.

[8] Koizumi K, Fujimoto H, Inokuchi H, Uchitsu M, Kono Y. Marine gravity measurements over the Seto Inland Sea, western Japan. Journal of the Geodetic Society of Japan 1994; 40: 333-345.

[9] Ohno I, Kono Y, Fujimoto H, Koizumi K. Gravity anomaly in and around the western Seto Inland Sea and subsurface structure of negative anomaly belt. Zisin (Bulletin of the Seismological Society of Japan) 1994; 47: 395-401.

[10] Kusumoto S, Fukuda Y, Takemoto S, Yusa Y. Three-dimensional subsurface structure in the eastern part of the Beppu-Shimabara Graben Kyushu, Japan, as revealed by gravimetric data. Journal of the Geodetic Society of Japan 1996; 42: 167-181.

[11] Davis PJ, Rabinowitz P. Methods of Numerical Integration, Second Edition. New York: Dover; 2007.

[12] Talwani M, Lamar WJ, Landisman M. Rapid gravity computations for two-dimensional bodies with application to the Mendocino Submarine Fracture Zone. Journal of Geophysical Research 1959; 64: 49-59.

[13] Yamada N, Teraoka Y, Hata M. Geological Atlas of Japan. Tsukuba: Geological Survey of Japan; 1982.

[14] Research Group for Active Faults. The Active Faults in Japan: Sheet Maps and Inventories Rev. Ed. Tokyo: Univ. of Tokyo Press; 1991.

[15] Wangen M. Physical Principles of Sedimentary Basin Analysis. London: Cambridge University Press; 2010.

[16] Geological Survey of Japan, AIST, editor. Seamless Digital Geological Map of Japan 1: 200,000 (July 3, 2012 Version), Research Information Database DB084. Tsukuba: National Institute of Advanced Industrial Science and Technology; 2012.

[17] Nagai K. Geology of the Ehime Prefecture. Matsuyama: Tomoeya; 1957.

[18] Ogawa M, Okamura M, Shimazaki K, Nakata T, Chida N, Nakamura T, Miyatake T, Maemoku H, Tsutsumi H. Holocene activity on a submarine active fault system of the Median Tectonic Line beneath the northeastern part of Iyonada, the Inland Sea, Southwest Japan. Memoir of the Geological Society of Japan 1992; 40: 75-97.

[19] Mizuno K. Preliminary report on the Plio-Pleistocene sediments distributed along the Median Tectonic Line in and around Shikoku, Japan. Bulletin of the Geological Survey of Japan 1987; 38: 171-190.

[20] Kitabayashi E, Danhara T, Iwano H. Fission-track age of zircon from volcanic ash layer of the Gunchu Formation in Iyo City, Ehime Prefecture in Shikoku, Japan. Journal of the Geological Society of Oita 2012; 18: 61-64.

[21] Nakagawa K, Ryoki K, Muto N, Nishimura S, Ito K. Gravity anomaly map and inferred basement structure in Osaka Plain, central Kinki, south-west Japan. Journal of Geosciences, Osaka City University 1991; 34: 103-117.

[22] Komazawa M, Ohta Y, Shibuya S, Kumai M, Murakami M. Gravity survey on the sea bottom of Osaka Bay and its subsurface structure. Butsuri-Tansa (Geophysical Exploration) 1996; 49: 459-473.

[23] Kusumoto S, Fukuda Y, Takemura K, Takemoto S. Forming mechanism of the sedimentary basin at the termination of the right-lateral left-stepping faults and tectonics around Osaka Bay. Journal of Geography 2001; 110: 32-43.

[24] Disaster Prevention Research Institute. Integrated Research Project for the Uemachi Active Fault System by METI. Uji: DPRI, Kyoto University; 2011.

[25] Osaka Prefecture. Subsurface Structural Survey of the Osaka Plain in the Heisei 15 Fiscal Year. http://www.hp1039.jishin.go.jp/kozo/osaka8frm.htm (accessed 22 March 2013).

[26] Nakatsuka T, Okuma S. Aeromagnetic Anomalies Database of Japan, Digital Geoscience Map P-6. Tsukuba: Geological Survey of Japan; 2005.

[27] Miyachi Y, Tainosho Y, Yoshikawa T, Sangawa A. Geology of the Osaka-Tonanbu District, with Geological Sheet Map at 1:50,000. Tsukuba: Geological Survey of Japan; 1998.

[28] Hoshi H, Tanaka D, Takahashi M, Yoshikawa T. Paleomagnetism of the Nijo Group and its implication for the timing of clockwise rotation of southwest Japan. Journal of Mineralogical and Petrological Sciences 2000; 95: 203-215.

[29] Talwani M, Ewing WM. Rapid computation of gravitational attraction of three-dimensional bodies of arbitrary shape. Geophysics 1960; 25: 203-225, doi: 10.1190/1.1438687.

[30] Talwani M. Computation with the help of a digital computer of magnetic anomalies caused by bodies of arbitrary shape. Geophysics 1965; 5: 797-817.